Biosensors and Bioelectronics 128 (2019) 159–165

Contents lists available at ScienceDirect

Biosensors and Bioelectronics

journal homepage: www.elsevier.com/locate/bios

Integrating an *ex-vivo* skin biointerface with electrochemical DNA biosensor for direct measurement of the protective effect of UV blocking agents

Seyedeh Zeinab Mousavisani[a,b], Jahan-Bakhsh Raoof[b], Kwan Yee Cheung[a], Aura Rocío Hernández Camargo[c,d,e], Tautgirdas Ruzgas[c,e], Anthony P.F. Turner[a,1], Wing Cheung Mak[a,*]

[a] Biosensors and Bioelectronics Centre, Department of Physics, Chemistry and Biology (IFM), Linkoping University, 58183 Linkoping, Sweden
[b] Eletroanalytical Chemistry Research Laboratory, Department of Analytical Chemistry, Faculty of Chemistry, University of Mazandaran, Babolsar, Iran
[c] Department of Biomedical Science, Faculty of Health and Society, Malmö University, SE-205 06 Malmö, Sweden
[d] Investigación en procesos de transformación de materiales para la industria farmacéutica, Departamento de Farmacia, Universidad Nacional de Colombia, Sede Bogotá, Colombia
[e] Biofilms - Research Center for Biointerfaces, Malmö University, SE-205 06 Malmö, Sweden

ARTICLE INFO

Keywords:
Skin biointerface
Electrochemical DNA biosensor
DNA damage
Nanoparticles
Sunscreens

ABSTRACT

Skin cancer is the most frequent kind of cancer in white people in many parts of the world. UV-induced DNA damage and genetic mutation can subsequently lead to skin cancer. Therefore development of new biosensing strategies for detection of UV-induced DNA damage is of great importance. Here we demonstrate a novel combination of an *ex-vivo* skin biointerface and an electrochemical DNA sensor for the direct detection of UV induced DNA damage and investigation the protective effect of various UV blockers (Zinc-oxide (ZnO), titanium-dioxide (TiO_2) nanoparticles (NPs) and sunscreens) against DNA damage. A diazonium modified screen-printed carbon electrode immobilized with a DNA sequence related to the p53 tumour suppressor gene, the most commonly affected gene in human UV-induced skin cancer, was applied as an electrochemical DNA sensor. Electrochemical impedance spectroscopy (EIS) was employed for the detection of DNA damage induced by UV-A radiation by following the changes in charge transfer resistance (R_{ct}). The protective effects of UV blockers applied onto a pig skin surface (a suitable model representing human skin) were successfully detected by the DNA sensor. We observed that the naked skin has little UV protection showing an 18.2% decreases in $\Delta R/R$ values compared to the control, while applying both NPs and NP-formulated sunscreens could significantly reduce DNA damage, resulting in a decrease in $\Delta R/R$ values of 67.1% (ZnO NPs), 77.2% (TiO_2 NPs), 77.1% (sunscreen 1) and 92.4% (sunscreen 2), respectively. Moreover, doping moisturising cream with NPs could provide a similar DNA protective effect. This new method is a biologically relevant alternative to animal testing and offers advantages such as fast, easy and inexpensive processing, in addition to its miniaturised dimension, and could be used for a range of applications in other sources of DNA damage and the protective effect of different UV blocking agents and other topical formulations.

1. Introduction

The skin is the largest organ of the body and accounts for almost 16% of body mass (Simões et al., 2015). Human skin is frequently exposed to ultraviolet radiation (UVR) that can result in various types of DNA damage. UVR consists of three main components: UV-C (200–280 nm), the most energetic UVR, which is absorbed by ozone and atmospheric oxygen and so generally does not reach the Earth's surface. Accordingly, the human population is mainly exposed to longer wavelength UV-B (290–320 nm) and UV-A (320–400 nm) radiation (Ikehata et al., 2008). UVA accounts for almost 95% of all the solar UVR that reaches the Earth and most probably is responsible for human skin cancer risk (Brem et al., 2017), in contrast to UVB, which constitutes about 5% of the solar UVR and can induce direct photo damage on DNA following absorption by DNA nucleobases (Brem et al., 2017).

Skin cancers are the most common malignancy of humans, particularly in white people, with over a million cases recognised annually (D'Orazio et al., 2013; Geller and Annas, 2003; Rogers et al., 2010).

* Corresponding author.
E-mail address: wing.cheung.mak@liu.se (W.C. Mak).
[1] Current address: SATM, Cranfield University, Bedfordshire, MK430AL, UK.

https://doi.org/10.1016/j.bios.2018.12.025
Received 23 November 2018; Accepted 10 December 2018
Available online 18 December 2018
0956-5663/

Induction of various types of DNA damage to cyclobutane pyrimidine dimers, pyrimidine (6-4) pyrimidone photoproducts, and other minor lesions is the first step in skin carcinogenesis induced by UV. Efficient action of various cellular repair systems that eliminate DNA lesions plays an important role in the inhibition of tumour formation (Ananthaswamy et al., 1998). The unfixed lesions may also interrupt cellular processes by blocking the DNA and RNA synthesising machineries and insert wrong bases into the DNA. Such mutation can lead to loss or inappropriate expression of the affected genes.

p53 tumour suppressor gene is by far the most commonly affected gene in human and mouse UV-induced skin cancers (Nataraj et al., 1995). It has been suggested that p53 acts as a "guardian of the genome" (Efeyan and Serrano, 2007) by helping DNA repair or causing deletion of cells with extreme DNA damage. Some studies indicates that the UV induced p53 mutations are an early occurrence in UV carcinogenesis and can act as a molecular marker for prior of solar exposure in humans (Ananthaswamy et al., 1997)

Sunscreens are widely used to protect the skin against the detrimental effects of UV-B and UV-A radiation (Smijs and Pavel, 2011). Sunscreens can reduce UV-induced DNA damage (Cayrol et al., 1999; Smijs and Pavel, 2011) and they are highly protective against sunburn and can reduce UV-induced skin aging (McCullough and Kelly, 2006) and the development skin cancer (Olsen et al., 2015). Zinc-oxide (ZnO) and titanium-dioxide (TiO_2) nanoparticles (NPs) are the most commonly used active ingredients in sunscreens due to their broad spectrum protection from UVR (absorption, reflection and scattering) (Monteiro-Riviere et al., 2011; Nasu and Otsubo, 2007; Smijs and Pavel, 2011). There is a considerable body of research that shows the blocking effect of ZnO and TiO_2 NPs against UVR (Cayrol et al., 1999; Nasu and Otsubo, 2007; Popov et al., 2005; Rouabhia et al., 2002).

Various methods such as high performance liquid chromatography (HPLC) (Su et al., 2010), single cell gel electrophoresis (SCGE) (Sastre et al., 2001), ^{32}p-postlabelling (Katiyar, 2013), fluorescence (O'donovan et al., 2005), chemiluminescence (Sinha et al., 2001) and electrochemical biosensors (Ferancová et al., 2010; Hlavata et al., 2012, 2015; Svitkova et al., 2017; Wang et al., 1997) have been applied to detect UV-induced DNA damage. In addition, different biological studies have been carried out to investigate the protective effect of sunscreens (Cayrol et al., 1999; Mouret et al., 2011; Reble et al., 2017; Rouabhia et al., 2002) and ZnO and TiO_2 (Nasu and Otsubo, 2007; Popov et al., 2005) against DNA damage, as well as detection of the UV induced DNA damages following UV irradiation to the skin (Ikehata et al., 2008). However, there is an absence of a link between analytical methods and biological skin models for effectively measuring the bioprotective effects of various agents against DNA damage.

Here, we introduce a new approach integrating an *ex-vivo* skin biointerface with an electrochemical DNA sensor for direct measurement on the protective effect of various agents (e.g. ZnO NPs, TiO_2 NPs and sunscreen creams) against UV induced DNA damage through a skin layer. Pig ear skin was chosen for the system as it represents a suitable model for human skin (Reble et al., 2017; Weigmann et al., 2009). DNA sensors immobilised with a p53 sequence, the most commonly affected gene in human UV-induced skin cancers, were incorporated underneath a skin layer to which the testing samples could be applied. We monitored the UV induced DNA damage by EIS, while the sensor was irradiated by UV A radiation through the skin layer. We have successfully demonstrated that the bare skin has an insignificant UV protection effect, while the application of ZnO and TiO_2 NPs, as well as sunscreens onto skin surface could protect against DNA damage.

2. Experimental section

2.1. Materials and instrumentation

Tetrafluoroboric acid solution, sodium nitrite 99.5%, 4-aminobenzoic acid, N-ethyl-N'-(3 dimethylaminopropyl) carbodiimide hydrochloride (EDC), N-hydroxysuccinimide (NHS), potassium ferricyanide (III), potassium ferrocyanide (II), sulphuric acid (H_2SO_4), titanium (IV) oxide (TiO_2) nanopowder (99.9%,) and zinc-oxide nanoparticle (ZnO) dispersion, 50 wt% in water (< 100 nm (DLS) particle size, < 35 nm average particle size) were purchased from Sigma–Aldrich (USA).

4-Aminobenzoic acid tetrafluoroborate, diazonium salt, were prepared according to our previous work (Mousavisani et al., 2018a).

ZnO and TiO_2 suspension with a concentration of 11 wt% in 0.1 M PBS (PH 7.4) were prepared and sonicated for 5 min. The nanoparticle suspensions were stored at 4 °C in the dark.

The creams used in this proof of principle are listed below:

Normal cream, moisturising cream: Dove intensive nourishing lotion,

Sunscreen 1: Ultra sensitive tint SPF 30, Dermalogica, Inc (which includes TiO_2 NPs 11.0 wt%).

Sunscreen 2: Skin perfect primer SPF 30, Dermalogica, Inc (which includes TiO_2 NPs 4.0 wt% and ZnO NPs 14.0 wt%)

The amine terminated DNA sequences related to the p53 gene used as a probe and its complementary target sequence, were purchased from biomers.net (Germany) and had the following sequence.

Amine terminated DNA: 5'-NH_2-GAGGTTGTGAGGCGCTGCCCCCA CCATG-3'

Stock solutions of DNA (100 μM) were prepared by dissolution in an appropriate amount of MilliQ water and stored in −20 °C. More diluted DNA solutions (1.0 μM) were obtained by using of 0.1 M of Tris-HCl containing 0.1 NaCl and stored in 4 °C.

A high intensity UV lamp (UVP, Upland, CA, USA), with a power of 100 W and working wavelength 365 nm, was used for UV radiation.

Voltammetric and impedimetric experiments were performed using an Ivium Stat XR electrochemical analyser equipped with commercial software (Ivium, Eindhoven, Netherlands) at ambient temperature. Screen-printed carbon electrodes (SPCEs) were obtained from Dropsens, Spain (Manufacturer code DRP-110). They comprise a carbon working electrode (diameter = 4 mm); a silver reference electrode and a carbon counter electrode printed onto a ceramic substrate.

Cyclic voltammetry (CV) was carried out over the potential range +0.5 to −0.3 V at a scan rate of 50 mV s^{-1} in 0.10 M Tris buffer solution (TBS) (pH 7.0) consisting of 0.1 M KCl and 5 mM $K_3[Fe(CN)_6]$/$K_4[Fe(CN)_6]$ (1:1) mixture.

Electrochemical impedance spectroscopy (EIS) was performed over a frequency range of 0.05 Hz–100 kHz at a 0 V bias potential vs. the open circuit potential (OCP) with an amplitude of 5 mV in the same solution that was used for CV measurements. All of the experiments were repeated for three times.

Contact angle measurements were performed using a CAM200 Optical Contact Angle Meter (KVS Instrument, Finland). An aliquot of 3 μL of fresh Milli Q water (18.2 MΩ) was placed onto bare SPCE, ACOOH/SPCE and DNA/ACOOH/SPCE and three images were recorded for each case.

Optical microscopy images were recorded using a light microscope (Zeiss Axio Vert. A1, Oberkochen, Germany) connected to a CCD colour digital camera (AxioCam Cm, Zeiss, Germany) and using the accompanying imaging software (Zen2012 blue edition, Zeiss, Germany).

2.2. Preparation of the DNA sensors

The diazonium salt-modified SPCE (ACOOH/SPCE) was obtained by dropping casting 100 μL of 5 mM of diazonium solution in 0.5 M cold sulphuric acid and applying 10 sequential potential sweeps from 0 to −1 V at a scan rate of 0.2 V s^{-1} (Ho et al., 2010). After the electrografting of the diazonium salt, the SPCEs were sonicated for 1 min in water to remove the weakly bound diazonium molecules, and slowly dried under a N_2 stream. Then, the COOH groups of the electrografted diazonium were activated by dropping 10 μL of 200 mM EDC and 50 mM NHS in water, onto electrode surfaces for 30 min. After washing

the electrodes with water and drying under a N_2 stream, 10 µL of aminated DNA (1.0 µM) was incubated on the activated electrode surface for 60 min. After that, the modified electrodes were incubated with 10 µL of 1 mM ethanolamine (pH 8), for half an hour to block unreacted COOH groups. Finally, the modified electrodes were rinsed with water and used for electrochemical experiments.

2.3. Preparation of skin membranes

Fresh pig ears were obtained from a local abattoir and stored at −80 °C if not immediately used. To prepare skin membranes, fresh or defrosted pig ears were rinsed with cold water and cut into strips with a scalpel. The outer part of the strip was shaved and approximately 500 µm thick skin membranes were sliced with a dermatome. The resulting skin strips were punched out to make circular membranes with 16 mm in diameter (details shown in supporting video). The membranes were stored in the fridge (−20 °C) on a filter paper soaked with PBS. Skin membranes, prepared as described, were used within two weeks (Nocchi et al., 2017).

2.4. Integration of skin membrane with electrochemical DNA sensors

The DNA sensor was placed in close proximity underneath the skin model, which was composed of a thin glass substrate (~0.2 mm) (Sub), a 1% (w/v) agarose hydrogel layer (~1 mm) (Gel), and a skin layer (Skin) separated by a PDMS spacer (~1 mm) to avoid contamination of the sensor surface (Fig. S1). The thin glass substrate provides a solid support to hold the skin layer, while the hydrogel layer retains the moisture of the skin layer during the experiment.

2.5. Damage of DNA by UV irradiation

The DNA/ACOOH/SPCE surface was exposed to irradiation with UV lamp for 40 min (as an optimum time) from 10 cm light source distance. After the exposure, the DNA/ACOOH/SPCE was rinsed with water and the subsequent electrochemical measurements (EIS, CV) were performed under the conditions detailed in Section 2.1. For impedance data, the normalised R_{ct} values were expressed using the Eq. (1)

$$\frac{\Delta R}{R} = \left(R_{ct,t} - R_{ct,0} \right) / R_{ct,0} \quad (1)$$

where $R_{ct,t}$ and $R_{ct,0}$ are the obtained charge transfer resistance values after and before exposure of a DNA sensor to UV irradiation.

2.6. DNA protective effects of ZnO, TiO_2 NPs and sunscreens measured by DNA sensors

A 0.88 cm^2 piece of skin membrane was placed on top of the DNA sensor, covered by 20 µL of 11 wt% of nanoparticle suspension (i.e. ZnO and TiO_2) and allowed to incubate for 15 min at room temperature, followed by exposed to UV radiation for 40 min. After that, the DNA sensors were rinsed with water and the EIS plots were recorded to evaluate the protective effect of the nanoparticles against UV-induced DNA damage. To study the effect of sunscreen and nanoparticle-doped moisturising cream, a dose of 2 mg cm^{-2} of cream was applied to the skin layer according to the standard testing protocol (Faurschou and Wulf, 2007).

3. Result and discussion

3.1. Design and construction of the electrochemical sensor for detection of DNA damage with skin model

Scheme 1 (left) illustrates the biological events that occur when skin is exposed to UV radiation causing DNA damage under the skin tissue, and the effect of UV blockers on the skin surface to reduce the amount of DNA damage. Scheme 1 (right) illustrates the concept of integrating an *ex vivo* skin biointerface on top of an electrochemical DNA sensor for direct measurement of the effect of UV radiation-induced DNA damage under the skin layer, as well as the protective effect of various agents (e.g. ZnO NPs, TiO_2 NPs and sunscreens) applied onto a skin surface, where the UV-protection effect against p53 DNA damage was measured directly by a DNA sensor below the skin. In real practice, we apply sun blockers onto the skin surface to protect our inner tissue from UV damage. Therefore, the skin membrane is the most relevant biointerface for this study. This novel combination provides an *ex vivo* skin-coupled biosensing module to measure the effect of DNA damage under the skin layer in a manner configured similarly to the biological layout of skin tissue.

3.2. Characterisation of the DNA biosensor

The DNA biosensor fabrication was characterised by using of CV and EIS techniques. Fig. 1A and B indicates the cyclic voltammograms and the EIS spectra related to SPCE (a), ACOOH/SPCE (b) and DNA/ACOOH/SPCE (c), respectively.

There is a pair of redox peaks at bare SPCE (a) with anodic and cathodic peak currents of about 126.7 µA and −117.07 µA, and a peak-to-peak potential separation of about 0.14 V (curve a, Fig. 1A). As soon

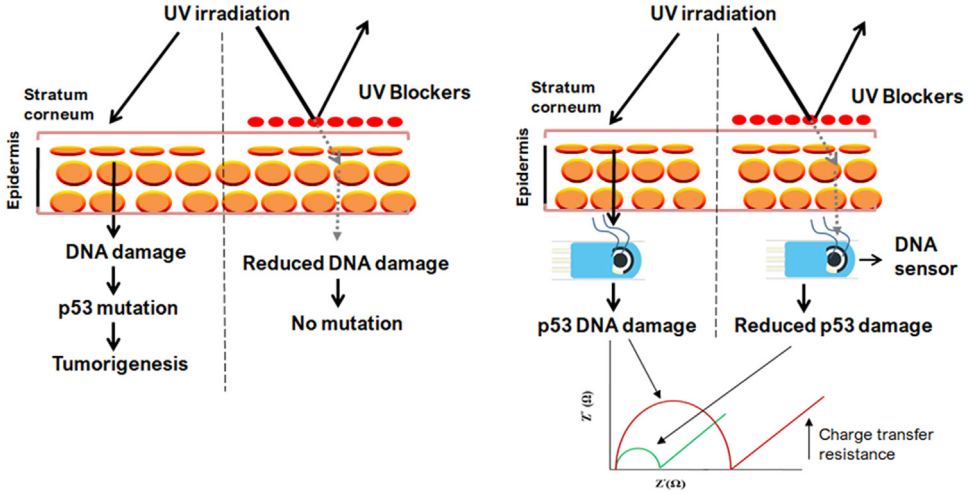

Scheme 1. Schematic illustration the detection principle on the protective effect of UV blockers against DNA damage.

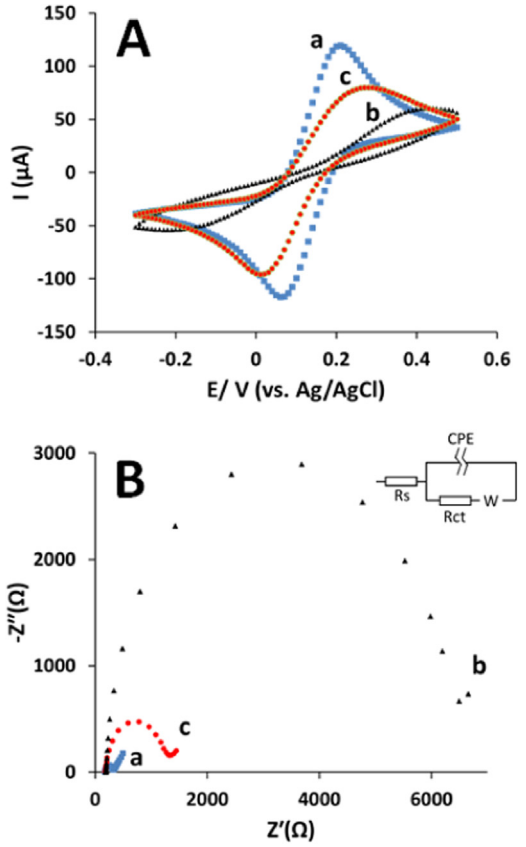

Fig. 1. (A) CVs of bare SPCE (a), ACOOH/SPCE (b) and DNA/ACOOH/SPCE (c) at scan rate 50 mV s^{-1}. (B) EIS spectra of bare SPCE (a), ACOOH/SPCE (b) and DNA/ACOOH/SPCE in 0.1 M TBS (pH 7.0) containing 0.1 M KCl and 5.0 mM $K_3[Fe(CN)_6]/K_4[Fe(CN)_6]$ (1:1) redox probe.

as the diazonium salt was electrografted on the SPCE surface, the anodic and cathodic peaks were largely disappeared (curve b, Fig. 1A). This result can be ascribed to the electrostatic repulsion force between the negatively charged carboxylic groups of the diazonium salt and $[Fe(CN)_6]^{3-/4-}$ which hinders the diffusion of $[Fe(CN)_6]^{3-/4-}$ to the electrode surface (Chung et al., 2012). Following DNA immobilisation on the surface of the ACOOH/SPCE, redox couple peaks were observed again (curve c, Fig. 1A), which can attributed to the less negative charge density of DNA compared to ACOOH and also the excess ACOOH being blocked following the ethanolamine treatment step (Bagheryan et al., 2016; Hayat et al., 2012; Mousavisani et al., 2018a). After the activation of electrode with diazonium salt, the ACOOH groups derived from the diazonium salt were activated by EDC/NHS forming a neutrally charged active NHS ester. Then, amine-functionalised DNA was coupled with the active NHS ester forming the DNA functionalised electrode. The intrinsic negative charge and high molecular weight of the amine-functionalised DNA molecules will affect the immobilisation efficiency leading to the formation of a relatively less dense DNA layer on the electrode surface. In contrast, electrodes without immobilised DNA remain capped by the neutrally charged active NHS ester. Therefore, the DNA/ACOOH/SPCE has a lower negative charge density compared with the ACOOH/SPCE. Moreover, neutralisation of the unreacted COOH groups was performed by ethanolamine treatment and led to a further decrease in the negative charge density of the DNA/ACOOH/SPCE than that of the ACOOH/SPCE (Bagheryan et al., 2016; Hayat et al., 2012; Mousavisani et al., 2018a).

EIS is one of the most informative methods in order to characterise electrochemical interfaces and it has acquired wide popularity as a direct and non-destructive method (Bandarenka, 2013) for studying interfacial properties such as charge transfer resistance. The diameter of the semicircle portion of the EIS spectra indicates the interfacial charge transfer resistance (Wang et al., 2004). All the obtained EIS spectra were fitted to the equivalent circuit indicated in the inset of Fig. 1B that consists of solution resistance (R_s), Warburg impedance (W), charge transfer resistance (R_{ct}) and constant phase element (CPE). Fig. 1B shows the EIS spectra obtained upon the stepwise modification process. As can be seen in this figure, a small semicircle with a R_{ct} of about 140 Ω characterised the bare SPCE (curve a). When the SPCE was modified with ACOOH, the R_{ct} increased to 6200 Ω (curve b). This increase can be related to formation of a high density of negatively charged diazonium film on the surface of electrode that was effectively preventing the diffusion of the $[Fe(CN)_6]^{3-/4-}$ redox couple to the sensor via electrostatic repulsion. After immobilisation of DNA on the surface of the modified electrode and treatment with ethanol amine, the R_{ct} value was dramatically decreased to 1079 Ω (curve c). This result is due to the lower negative charge density of DNA/ACOOH/SPCE than that of ACOOH/SPCE (explained in the CV studies) which could promote the diffusion of the $[Fe(CN)_6]^{3-/4-}$ redox couple to the electrode surface causing a decrease in R_{ct} value, which is in good agreement with CV studies (Bagheryan et al., 2016; Hayat et al., 2012). In addition, contact angle measurements were performed to characterise the step-wise fabrication of the DNA sensors. The average values of contact angles were calculated as 104.37° ± 0.71°, 31.42° ± 0.96° and 18.85° ± 0.86° for bare SPCE, ACOOH/SPCE and DNA/ACOOH/SPCE, respectively (Fig. S2). As the data shows, the contact angle decreased following grafting of diazonium salt and DNA immobilisation, indicating that the surface hydrophilicity was enhanced following the introduction of carboxylic groups and, subsequently, DNA molecules (Bagheryan et al., 2016). The contact angle measurements further confirm the successful preparation of the DNA sensor.

3.3. Electrochemical detection of UV induced DNA damage

Electrochemical methods including EIS and CV were applied to detect and evaluate the DNA damage which was induced by UV irradiation at the surface of the DNA sensor. The impedance spectra and cyclic voltammograms of the (a) as-prepared DNA sensor, and (b) DNA sensor without UV-illumination (UV-lamp off for 40 min) and (c) after UV-illumination (UV-lamp on for 40 min), are shown in Fig. 2A and B, respectively. Fig. 2A shows that in the absence of UV irradiation (curve b), there is no significant change in R_{ct} compared to the as prepared DNA sensor (curve a). While, following exposure of the DNA biosensor to UV irradiation, the charge transfer resistance dramatically increased from 1079 Ω (curve a), to 3362 Ω (curve c), indicating a decrease in the electron transfer rate between the $[Fe(CN)_6]^{3-/4-}$ molecules and the electrode as reported by other researchers (Chen et al., 2012; Mousavisani et al., 2018b; Xiong et al., 2013). UV irradiation can induce different types of DNA modifications such as single strand breaks (SSB), bipyrimidine photoproducts and oxidatively damaged bases (Douki et al., 2003; Girard et al., 2011). It appears that 8-oxo-7,8-dihydroguanine (8-oxoGua) is the main oxidatively induced DNA damage (Cadet et al., 2005). The oxidised DNA bases consist of electron rich carbonyl group and hydroxyl group, which cause an increase in electronegativity of the DNA structure that will decrease the accessibility of the negatively charged $[Fe(CN)_6]^{3-/4-}$ redox probe to the electrode surface resulting an increase in the R_{ct} (Mousavisani et al., 2018a). The EIS results were confirmed by the CV analysis of 5 mM of $[Fe(CN)_6]^{3-/4-}$ redox probe (Fig. 2B). As seen in this figure, the anodic and cathodic peak currents and the potential separation of the redox probe were similar for the (a) as prepared DNA sensor and (b) DNA sensor without UV-illumination (UV-lamp off for 40 min). In constrast, the anodic and cathodic peak currents of the redox probe were clearly decreased and the potential separation was increased for (c) the irradiated DNA sensor compared to (a) the non-irradiated DNA sensor illustrating that the rate of electron transfer between redox probe and the electrode was decreased. With the control experiments, it is confirmed that UV

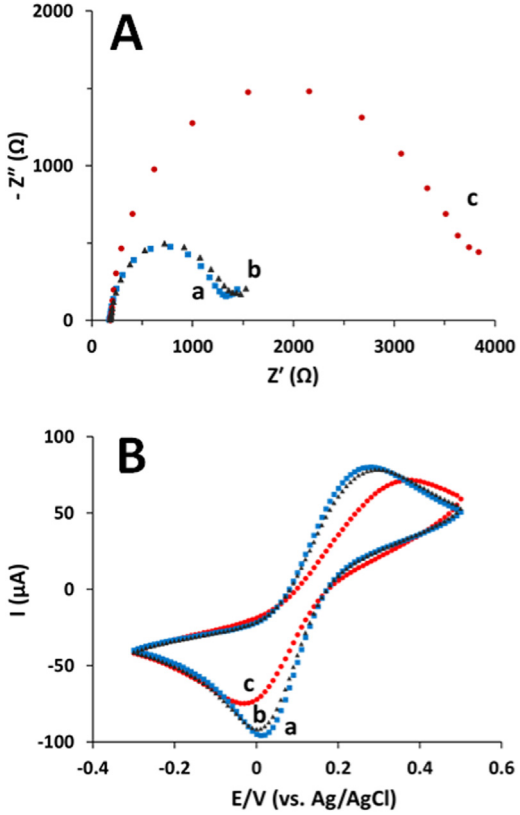

Fig. 2. (A) EIS spectra and (B) CVs of (a) as-prepared DNA sensor, and (b) DNA sensor without UV-illumination (UV-lamp off for 40 min) and (c) after UV-illumination (UV-lamp on for 40 min) in 0.1 M TBS (pH 7.0) containing 0.1 M KCl and 5.0 mM $K_3[Fe(CN)_6]/K_4[Fe(CN)_6]$ (1:1) redox probe.

irradiation is responsible for the responses (i.e. the observed changes in R_{ct} or in anodic and cathodic peak currents and potential separation).

3.4. Effect of irradiation time on the damage degree

To study the effect of irradiation time on damage degree, the corresponding dependences of the normalised EIS signals, ΔR/R (as defined in Section 2.5), on different exposure times (0–60 min) of the DNA/ACOOH/SPCE to UV radiation were recorded. Fig. 3A clearly shows that the ΔR/R value increased with increasing time of exposure to UV radiation and reached a maximum value after 40 min. Therefore, 40 min was chosen as an irradiation time for further experiments. Moreover, the effect of the irradiation time (40 min) on the morphology and integrity of the skin layer was investigated. Fig. 3B shows optical microscopy images of the skin before (Bi) and after (Bii) irradiation (40 min) illustrating the retention of similar cell surface morphology and hydration supported by the underlying hydrogel layer.

3.5. Skin biointerface integrated DNA sensors to study the protective effects of NPs against UV induced DNA damage

Experiments were performed with the set up described in the experimental section. Fig. 4A shows the normalised signal, ΔR/R, following UV irradiation of (a) the DNA sensor, or the DNA sensor in the presence of (b) Sub, (c) Sub/Gel, (d) Sub/Gel/Skin, (e) Sub/Gel/Skin + TiO_2 NPs (11 wt%) and (f) Sub/Gel/Skin + ZnO NPs (11 wt%) with corresponding ΔR/R of 1.97 ± 0.06, 1.92 ± 0.075, 1.83 ± 0.036, 1.61 ± 0.061, 0.65 ± 0.059 and 0.45 ± 0.025, respectively. The percentage decreases in ΔR/R value in the presence of Sub and Sub/Gel were 2.5% and 7.1% compared with the DNA sensor. This indicates that the Sub and Gel layers are relatively transparent to the applied UV and

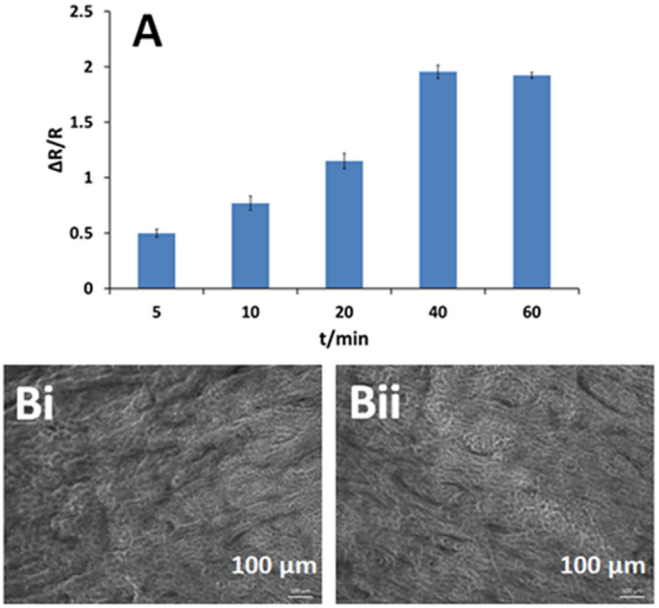

Fig. 3. (A) Effect of irradiation time on degree of damage in 0.1 M TBS (pH 7.0) containing 0.1 M KCl and 5.0 mM $K_3[Fe(CN)_6]/K_4[Fe(CN)_6]$ (1:1) redox probe. All of the experiments were carried out three times, (B) Optical microscopy images of the skin before (a) and after (b) 40 min irradiation time.

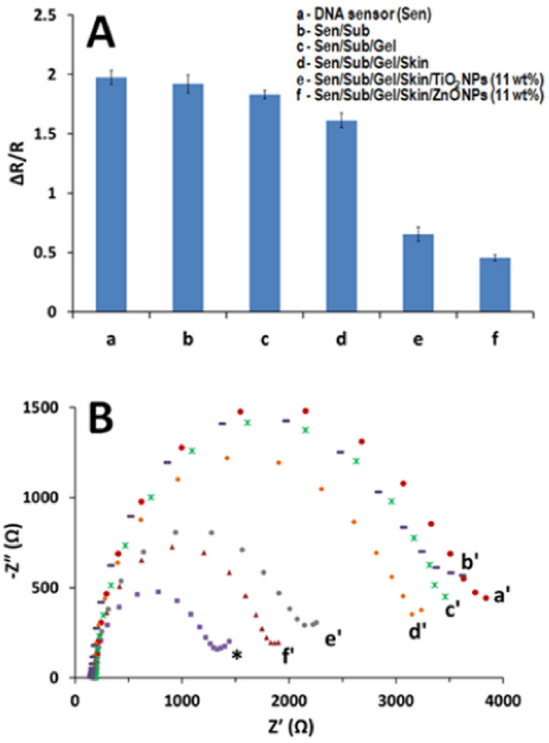

Fig. 4. (A) ΔR/R value following UV irradiation of (a) the DNA sensor, and corresponding control experiments in the presence of (b) Sub, (c) Sub/Gel, (d) Sub/Gel/Skin, (e) Sub/Gel/Skin + TiO_2NPs (11 wt%) and (f) Sub/Gel/Skin + ZnO NPs (11 wt%). (B) The EIS spectra of the DNA sensor (*) before UV irradiation, (a′) after UV irradiation and after UV irradiation in the presence of (b′) Sub, (c′) Sub/Gel, (d′) Sub/Gel/Skin, (e′) Sub/Gel/Skin + TiO_2NPs (11 wt %) and (f′) Sub/Gel/Skin + ZnO NPs (11 wt%) in 0.1 M TBS (pH 7.0) containing 0.1 M KCl and 5.0 mM $K_3[Fe(CN)_6]/K_4[Fe(CN)_6]$ (1:1) redox probe. All experiments were carried out three times.

have a minor effect on the measurement. In contrast, the percentage decreases in ΔR/R in the presence of the skin layer was 18.2%,

indicating a small UV is blocking effect by the skin. In contrast, we observed significant percentage decreases in ΔR/R values of 67.1% and 77.2% after the skin treated with (e) 11 wt% ZnO NPs and (f) 11 wt% TiO_2 NPs, respectively. These decreases indicate the protective effect of these NPs by blocking or absorption of UV-A and reduce the UV-A induced DNA damage of p53 at the sensor surface. As seen in Fig. 4A, ZnO showed a greater protective effect against UV than TiO_2, due to its more effective UV-A absorbance compared to TiO_2 (Beasley and Meyer, 2010; Pinnell et al., 2000; Smijs and Pavel, 2011). The EIS spectra of the DNA sensor (*) before UV irradiation, (a′) after UV irradiation and after UV irradiation in the presence of (b′) Sub, (c′) Sub/Gel, (d′) Sub/Gel/Skin, (e′) Sub/Gel/Skin + TiO_2NPs (11 wt%) and (f′) Sub/Gel/Skin + ZnO NPs (11 wt%) are shown in Fig. 4B with a responding R_{ct} of 1079 ± 6.0, 3362 ± 5.7, 3150 ± 4.23, 3049 ± 5.3, 2816 ± 2.28, 1780 ± 3.06 and 1564 ± 2.36 Ω, respectively. The R_{ct} value was significantly decreased in the presence of the skin layers which were treated by TiO_2 NPs (e′) and ZnO NPs (f′) due to the protective effect of these NPs by blocking or absorption of UV-A. This result showed that ZnO has more protective effect against UV than TiO_2, due to its more effective UV-A absorbance compared to TiO_2 (Beasley and Meyer, 2010; Pinnell et al., 2000; Smijs and Pavel, 2011).

3.6. Protective effects of NPs formulated commercial sunscreens and nanoparticle-doped moisturising cream on the skin model against UV induced DNA damage

Fig. 5A shows the calculated ΔR/R value following UV irradiation of the DNA sensor (a), DNA sensor in the presence of (b) Sub/Gel/Skin, (c) Sub/Gel/Skin + moisturising cream, (d) Sub/Gel/Skin + sunscreen 1, and (e) Sub/Gel/Skin + sunscreen 2 with responding values of 1.97 ± 0.059, 1.61 ± 0.061, 1.45 ± 0.050, 0.45 ± 0.030, 0.15 ± 0.032, respectively. The percentage decreases in ΔR/R value in the presence of Sub/Gel/Skin and Sub/Gel/Skin + moisturising cream were 18.2% and 26.4% compared with the DNA sensor. This indicates that the moisturising cream cannot significantly protect DNA against UV irradiation. In contrast, the percentage decreases in ΔR/R in the presence of the skin treated with sunscreens (d and e) were 77.1% and 92.4% which indicate reduced DNA damage due to their effective UV protective effect. The results indicate that the skin model was successful for investigation of the protective effect of sunscreens against UV induced DNA damage. Moreover, the EIS spectra of the DNA sensor (*) before and (a′) after UV irradiation, and following UV irradiation in the presence of (b′) Sub/Gel/Skin, (c′) Sub/Gel/Skin + moisturising cream, (d′) Sub/Gel/Skin + sunscreen 1, and (e′) Sub/Gel/Skin + sunscreen 2 are shown in Fig. 5B with corresponding R_{ct} of 1079 ± 6.0, 3362 ± 5.70, 2816 ± 2.28, 2643 ± 4.92, 1536 ± 2.73 and 1235 Ω ± 2.91, respectively. As seen, the R_{ct} value shows no significant change when the skin was treated with the moisturising cream (c′) in comparison with untreated skin (b′), indicating that the moisturising cream cannot significantly block UV radiation and thereby shows no substantial protective effect against DNA damage. While, the R_{ct} value was significantly decreased to (1536 ± 2.73 Ω, d′) and (1235 ± 2.91 Ω, e′), in the presence of skin treated with sunscreen 1 and sunscreen 2, respectively. These observations can be due to the UV blocking effect of sunscreens which included ZnO and TiO_2 NPs that could have a protective effect by reducing the DNA damage.

In addition, the protective effect of moisturising cream, which was doped with different concentration of ZnO and TiO_2NPs was investigated. For this purpose, the normalised signal, ΔR/R values following UV irradiation of the DNA sensor (a), and in the presence of (b) Sub/Gel/Skin, (c) Sub/Gel/Skin + moisturising cream, Sub/Gel/Skin + moisturising cream which was doped with: (d) 4 wt% TiO_2, (e) 11 wt % TiO_2, (f) 11 wt% ZnO, (g) 14 wt% ZnO, (h) 4 wt% TiO_2 + 14 wt% ZnO, were obtained as 1.97 ± 0.059, 1.61 ± 0.061, 1.45 ± 0.050, 0.94 ± 0.04, 0.74 ± 0.041, 0.55 ± 0.040, 0.46 ± 0.03, 0.33 ± 0.026, and were shown in Fig. 5C. The percentage decreases in

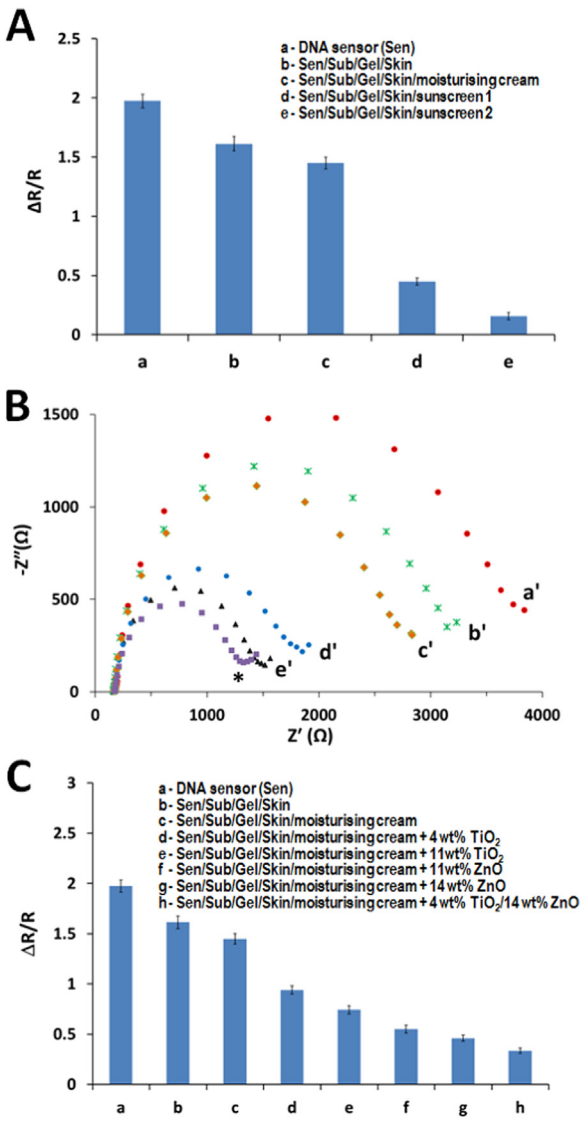

Fig. 5. (A), ΔR/R value following UV irradiation of the DNA sensor (a), DNA sensor in the presence of (b) Sub/Gel/Skin, (c) Sub/Gel/Skin + moisturising cream, (d) Sub/Gel/Skin + sunscreen 1, and (e) Sub/Gel/Skin + sunscreen 2. (B) The EIS spectra of the of the DNA sensor (*) before and (a′) after UV irradiation, and following UV irradiation in the presence of (b′) Sub/Gel/Skin, (c′) Sub/Gel/Skin + moisturising cream, (d′) Sub/Gel/Skin + sunscreen 1, and (f′) Sub/Gel/Skin + sunscreen 2 in 0.1 M TBS (pH 7.0) containing 0.1 M KCl and 5.0 mM $K_3[Fe(CN)_6]/K_4[Fe(CN)_6]$ (1:1) redox probe. (C) ΔR/R values following UV irradiation of the DNA sensor (a), the DNA sensor in the presence of (b) Sub/Gel/Skin, (c) Sub/Gel/Skin + moisturising cream, Sub/Gel/Skin + moisturising cream which doped with: (d) 4 wt% TiO_2, (e) 11 wt% TiO_2, (f) 11 wt% ZnO, (g) 14 wt% ZnO and (h) 4 wt% TiO_2 + 14 wt% ZnO. All experiments were carried out three times.

ΔR/R value in the presence of Sub/Gel/Skin + moisturising cream which was doped with 4% TiO_2, 11% TiO_2 and 11% ZnO, were 52%, 62% and 72%, respectively. This indicates that the protective effect of TiO_2 NPs is increased with increasing concentration and that the moisturising cream doped with 11% ZnO (f) provides a better protection compared to 11% TiO_2 (e) due to the fact that ZnO has more effective UV-A absorbance compared to TiO_2 (Beasley and Meyer, 2010; Pinnell et al., 2000; Smijs and Pavel, 2011). Moreover, by comparing Fig. 5B and C, it can be concluded that the doped moisturising creams with 11% TiO_2 with percentage decreases in ΔR/R value of 62% (e, Fig. 5C) and 4% TiO_2 + 14% ZnO with percentage decrease of 83% (h, Fig. 5C) have a less protective effect than sunscreen 1 with percentage

decrease of 77.1%, (d, Fig. 5B) and sun screen 2 with percentage decrease of 92.4%, (e Fig. 5B), respectively. This may due to the sunscreens contain other chemical component which has a protective effect against UV in comparison to the doped moisturising cream. The EIS spectra of the DNA sensor (*) before and (a′) after UV irradiation, and following UV irradiation in the presence of (b′) Sub/Gel/Skin, (c′) Sub/Gel/Skin + moisturising cream, (d′) Sub/Gel/Skin + moisturising cream + 4% TiO_2, (e′) Sub/Gel/Skin + moisturising cream + 11% TiO_2, (f′) Sub/Gel/Skin + moisturising cream + 11% ZnO, (g′) Sub/Gel/Skin + moisturising cream + 14% ZnO and (h′) Sub/Gel/Skin + moisturising cream + 4% TiO_2 + 14% ZnO are shown in Fig. S3.

4. Conclusions

We have demonstrated a novel and more clinically relevant strategy, based on a combination of a skin biointerface and an electrochemical DNA sensor, for the direct detection of UV induced DNA damage and the investigation of the protective effect of various skin creams containing UV blockers or other topical formulations. A skin layer was placed on top of an electrochemical DNA sensor and the UV blocking agents were applied on the skin surface to determine the level of DNA damage upon exposure to UV in a more biologically relevant and simple testing system. We successfully measured the DNA protective effect of various NPs and NP-formulated sunscreens applied onto a skin surface under UV illumination, and observed that both ZnO and TiO_2, and corresponding sunscreens could significantly reduce DNA damage as indicated by a strong decrease in the $\Delta R/R$ response (ranging between 67.1% and 92.4%) measured by the electrochemical DNA sensor. This novel skin interfaced DNA sensor could provide a new analytical tool for rapid and direct evaluation on the DNA protective effect of various UV-blocker applied onto skin surface.

Acknowledgement

T. Ruzgas acknowledges financial support from The Knowledge Foundation (grants: 20140211 and 20170058) and The Gustav Th. Ohlssons Fond.

Declaration of interests

None.

Appendix A. Supplementary material

Supplementary data associated with this article can be found in the online version at doi:10.1016/j.bios.2018.12.025.

References

Ananthaswamy, H.N., Loughlin, S.M., Cox, P., Evans, R.L., Ullrich, S.E., Kripke, M.L., 1997. Nat. Med. 3 (5), 510–514.
Ananthaswamy, H.N., Loughlin, S.M., Ullrich, S.E., Kripke, M.L., 1998. Inhibition of UV-induced p53 mutations by sunscreens: implications for skin cancer prevention. J. Investig. Dermatol. Symp. Proc 52–56.
Bagheryan, Z., Raoof, J.-B., Golabi, M., Turner, A.P., Beni, V., 2016. Biosens. Bioelectron. 80, 566–573.
Bandarenka, A.S., 2013. Analyst 138 (19), 5540–5554.
Beasley, D.G., Meyer, T.A., 2010. Am. J. Clin. Dermatol. 11 (6), 413–421.
Brem, R., Guven, M., Karran, P., 2017. Free Radic. Biol. Med. 107, 101–109.
Cadet, J., Sage, E., Douki, T., 2005. Mutat. Res./Fundam. Mol. Mech. Mutagen. 571 (1), 3–17.
Cayrol, C., Sarraute, J., Tarroux, R., Redoules, D., Charveron, M., Gall, Y., 1999. Br. J. Dermatol. 141 (2), 250–258.
Chen, Y., Xiong, H., Zhang, X., Wang, S., 2012. Microchim. Acta 178 (1–2), 37–43.
Chung, D.-J., Oh, S.-H., Komathi, S., Gopalan, A.I., Lee, K.-P., Choi, S.-H., 2012. Electrochim. Acta 76, 394–403.
D'Orazio, J., Jarrett, S., Amaro-Ortiz, A., Scott, T., 2013. Int. J. Mol. Sci. 14 (6), 12222–12248.
Douki, T., Reynaud-Angelin, A., Cadet, J., Sage, E., 2003. Biochemistry 42 (30), 9221–9226.
Efeyan, A., Serrano, M., 2007. Cell Cycle 6 (9), 1006–1010.
Faurschou, A., Wulf, H., 2007. Br. J. Dermatol. 156 (4), 716–719.
Ferancová, A., Rengaraj, S., Kim, Y., Labuda, J., Sillanpää, M., 2010. Biosens. Bioelectron. 26 (2), 314–320.
Geller, A.C., Annas, G.D., 2003. Epidemiology of melanoma and nonmelanoma skin cancer. Semin. Oncol. Nurs. 2–11 (Elsevier).
Girard, P., Francesconi, S., Pozzebon, M., Graindorge, D., Rochette, P., Drouin, R., Sage, E., 2011. UVA-induced damage to DNA and proteins: direct versus indirect photochemical processes. J. Phys.: Conf. Ser. 012002.
Hayat, A., Barthelmebs, L., Marty, J.-L., 2012. Sens. Actuator B-Chem. 171, 810–815.
Hlavata, L., Benikova, K., Vyskocil, V., Labuda, J., 2012. Electrochim. Acta 71, 134–139.
Hlavata, L., Striesova, I., Ignat, T., Blaskovisova, J., Ruttkay-Nedecky, B., Kopel, P., Adam, V., Kizek, R., Labuda, J., 2015. Microchim. Acta 182 (9–10), 1715–1722.
Ho, J.-aA., Hsu, W.-L., Liao, W.-C., Chiu, J.-K., Chen, M.-L., Chang, H.-C., Li, C.-C., 2010. Biosens. Bioelectron. 26 (3), 1021–1027.
Ikehata, H., Kawai, K., Komura, J.-I., Sakatsume, K., Wang, L., Imai, M., Higashi, S., Nikaido, O., Yamamoto, K., Hieda, K., 2008. J. Investig. Dermatol. 128 (9), 2289–2296.
Katiyar, S.K., 2013. Green Tea Polyphenols: Nutraceuticals of Modern Life. pp. 119.
McCullough, J.L., Kelly, K.M., 2006. Ann. N. Y. Acad. Sci. 1067 (1), 323–331.
Monteiro-Riviere, N., Wiench, K., Landsiedel, R., Schulte, S., Inman, A., Riviere, J., 2011. Toxicol. Sci. 123 (1), 264–280.
Mouret, S., Bogdanowicz, P., Haure, M.J., Castex-Rizzi, N., Cadet, J., Favier, A., Douki, T., 2011. Photochem. Photobiol. 87 (1), 109–116.
Mousavisani, S.Z., Raoof, J.-B., Turner, A.P., Ojani, R., Mak, W.C., 2018a. Sens. Actuator B-Chem.
Mousavisani, S.Z., Raoof, J.B., Ojani, R., Bagheryan, Z., 2018b. Bioelectrochemistry 122, 142–148.
Nasu, A., Otsubo, Y., 2007. J. Colloid Interface Sci. 310 (2), 617–623.
Nataraj, A.J., II, J.C.T., Ananthaswamy, H.N., 1995. Photochem. Photobiol. 62 (2), 218–230.
Nocchi, S., Björklund, S., Svensson, B., Engblom, J., Ruzgas, T., 2017. Biosens. Bioelectron. 93, 9–13.
O'donovan, P., Perrett, C.M., Zhang, X., Montaner, B., Xu, Y.-Z., Harwood, C.A., McGregor, J.M., Walker, S.L., Hanaoka, F., Karran, P., 2005. Science 309 (5742), 1871–1874.
Olsen, C.M., Wilson, L.F., Green, A.C., Bain, C.J., Fritschi, L., Neale, R.E., Whiteman, D.C., 2015. Aust. N. Z. J. Public Health 39 (5), 471–476.
Pinnell, S.R., Fairhurst, D., Gillies, R., Mitchnick, M.A., Kollias, N., 2000. Dermatol. Surg. 26 (4), 309–314.
Popov, A., Priezzhev, A., Lademann, J., Myllylä, R., 2005. J. Phys. D 38 (15), 2564.
Reble, C., Gersonde, I., Schanzer, S., Meinke, M.C., Helfmann, J., Lademann, J., 2017. J. Biophotonics.
Rogers, H.W., Weinstock, M.A., Harris, A.R., Hinckley, M.R., Feldman, S.R., Fleischer, A.B., Coldiron, B.M., 2010. Arch. Dermatol. 146 (3), 283–287.
Rouabhia, M., Mitchell, D.L., Rhainds, M., Claveau, J., Drouin, R., 2002. Photochem. Photobiol. Sci. 1 (7), 471–477.
Sastre, M.P., Vernet, M., Steinert, S., 2001. Photochem. Photobiol. 74 (1), 55–60.
Simões, M., Sousa, J., Pais, A., 2015. Cancer Lett. 357 (1), 8–42.
Sinha, R.P., Dautz, M., Hader, D., 2001. Acta Protozool. 40 (3), 187–196.
Smijs, T.G., Pavel, S., 2011. Nanotechnol. Sci. Appl. 4, 95.
Su, D.G., Taylor, J.-S.A., Gross, M.L., 2010. Chem. Res. Toxicol. 23 (3), 474–479.
Svitkova, V., Blaskovicova, J., Tekelova, M., Kallai, B.M., Ignat, T., Horackova, V., Skladal, P., Kopel, P., Adam, V., Farkasova, D., 2017. Sens. Actuator B-Chem. 243, 435–444.
Wang, J., Rivas, G., Ozsoz, M., Grant, D.H., Cai, X., Parrado, C., 1997. Anal. Chem. 69 (7), 1457–1460.
Wang, M., Wang, L., Wang, G., Ji, X., Bai, Y., Li, T., Gong, S., Li, J., 2004. Biosens. Bioelectron. 19 (6), 575–582.
Weigmann, H.-J., Schanzer, S., Patzelt, A., Bahaban, V., Durat, F., Sterry, W., Lademann, J., 2009. J. Biomed. Opt. 14 (2) (024027-024027-024026).
Xiong, H., Chen, Y., Zhang, X., Gu, H., Wang, S., 2013. Sens. Actuator B-Chem. 181, 85–91.